A New Ultrafast Thermometer for Airborne Measurements in Clouds

KRZYSZTOF E. HAMAN, ANDRZEJ MAKULSKI, AND SZYMON P. MALINOWSKI

Warsaw University, Warsaw, Poland

REINHOLD BUSEN

DLR Oberpfaffenhofen, Wessling, Germany

(Manuscript received 21 August 1995, in final form 10 July 1996)

ABSTRACT

A new aircraft device for measuring temperature in clouds is described. Its sensor is a resistance thermometer made of platinum-coated tungsten wire 5 mm long and 2.5 μm in diameter. The sensor is located on a rotatable vane behind a thin rod aimed at protecting it against the impact of cloud droplets, which according to limited experience gathered until now seems to be sufficiently effective as an antiwetting protection for the speeds of motorgliders. Contrary to the massive housings usually adopted in other constructions, the rod creates only negligible disturbances in the thermodynamic properties of the ambient air. The time constant of the sensor is of the order 10^{-4} s, which permits measurements of temperature in clouds with a resolution of a few centimeters, depending on aircraft velocity. The thermometer was tested in a wind tunnel, and on an Ogar motorglider and a Do-228 aircraft. Its present version performs fairly well at low airspeeds of up to about 40 m s^{-1}. For faster aircraft further improvements seem necessary. The paper presents a detailed description of the instrument, discussion of test results, and examples of centimeter-scale features of temperature fields in clouds measured with the thermometer.

1. Introduction

Accurate measurement of temperature in clouds, especially on a very small scale, is still a formidable task. For noncontact radiometric instruments the main difficulty is connected with the relatively large volume of the air sample (Lawson and Cooper 1990). Acoustic instruments (Marillier et al. 1991) seem basically unsuitable for cloud measurements, because in cloudy air the dependence of the speed of sound on temperature is ill determined. For contact (immersion) thermometers the question consists of protecting the sensing element from the impact of cloud droplets without disturbing the measurement. The relatively large and massive housings used for that purpose in the most popular aircraft resistance thermometers (Rosemount, ''reverse flow,'' NCAR K) create considerable problems in that respect. Rosemount (1963), Rodi and Spyers-Duran (1972), Lenschow (1972), McCarthy (1973), and Parathoen et al. (1982) have shown that the thermal effects of the housing and supports result in considerably slowing down the response of the instrument. The relaxation curve may be approximated by a linear combination of two exponential functions with two time constants, one corresponding to the response of the instrument and the second, much longer, to the response of the housing and supports. Friehe and Khelif (1993), who systematically investigated the response of standard Rosemount sensor versus a fine-bead thermistor in the Rosemount housing and NCAR K thermometric probe, found that such a two-time-constant representation of the instrument response is fairly good, but for their fastest instrument its approximation by one exponential curve with ''average'' time constant equal to 0.148 at 70 m s^{-1} is also acceptable. The new thermocouple instrument described by Lawson and Rodi (1992) might be better in that respect than the Rosemount or the reverse flow. Its time constant is difficult to estimate from the published data, which involve the effects of filtering by the recording system, but for its sensor—a thermocouple made of 12.5-μm wire—it can hardly be less than 10^{-2} s. Similar values can be expected for improved versions of the VTU-1 thermocouple sensor (Haman 1992) and this seems to be the limit for the present design. This means that even for a very slow aircraft (30 m s^{-1}) thermal structures smaller than 1–2 m will be recorded with considerable distortions. Some improvement can be achieved by numerical processing of the measured time series (Shaw and Tillman 1980), but in the case of a

Corresponding author address: Dr. Krzysztof Haman, Institute of Geophysics, University of Warsaw, Pasteura 7, Warsaw UL. 02-093, Poland.
E-mail: khaman@mimuw.edu.pl

high noise-to-signal ratio, the possibilities of this method are rather limited.

Another problem with large housings is that in clouds the thermodynamics of the airflow around the sensor is strongly distorted with respect to the case of the unprotected sensor located far from the aircraft body. Wrong localization of the sensor within the airflow disturbances created by the aircraft may be a source of additional distortions. Exchange of latent heat with the water collected on the sensor housing or the aircraft parts affects the character of local pressure changes that may not be purely dry nor purely wet adiabatic, and their thermal effects may depend randomly on the cloud spectrum and flight parameters. This creates great difficulties with determination of the effective value of recovery factor. Its value determined from measurements in dry air may appear unapplicable (Lawson and Cooper 1990; Nacass 1992) and in fact, may become unpredictable. For airspeeds of 30 m s^{-1}, characteristic for a motorglider, this effect might be negligible, but for faster aircraft it may yield intolerable errors. The recent study by Fuehrer et al. (1994) seems to confirm this conclusion.

On the other hand, there is increasing evidence that mixing processes in clouds create small-scale inhomogeneities of thermodynamical properties that may play a major role in determining the behavior and evolution of clouds (see, e.g., Baker 1992; Grabowski 1993; Malinowski et al. 1994; Haman and Pawlowska 1995). Thus, in-cloud measurements of thermodynamical fields that reveal small-scale features down to centimeter scale are important. The first steps have been made with respect to distribution of droplets with use of improved forward scattering spectrometer probes (FSSP) (Baumgardner et al. 1993; Brenguier 1993). This paper presents similar attempts with respect to the temperature field.

To make high-resolution measurements of temperature, a new fast, immersion aircraft temperature sensor for clouds has been developed. It is designated as UFT, for ultrafast thermometer. Its basic construction is similar to that of the airborne thermocouple sensor VTU-1 described by Haman (1992) but involves a number of changes and improvements. The main change is replacing the thermocouple with an ultrafine resistance wire characterized by time constant of the order of 10^{-4} s. The antidroplet shield, similar to that in the VTU-1, is very small and affects the measurement only to a marginal degree. This means that features of the temperature field of a size as small as 3–5 cm should be detectable by this instrument directly, without major distortions; with some computational correction procedures even the 1-cm limit seems possible.

In the following, the design of the present version of the instrument is described, and results of laboratory and in-flight tests are discussed as well as directions for its further development. Finally, examples of some measurements made in cumulus clouds with this instrument are presented as an illustration of its capabilities.

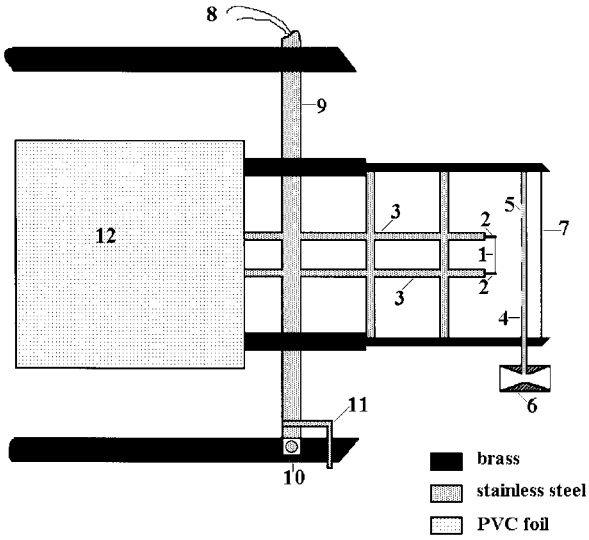

FIG. 1. Schematic view of the UFT sensor: (1) sensing element (tungsten wire, diameter 2.5 μm, length 5 mm); (2) Teflon-insulated copper supports; (3) stainless-steel tubes; (4) protecting rod made of stainless steel; (5) holes for water removal from the rod; (6) Venturi nozzle for water removal; (7) protective nylon thread; (8) copper connectors; (9) shaft; (10) ball-point bearing; (11) shaft stops; (12) vane.

2. Construction of the sensor

The basic design of the key mechanical components of the UFT thermometric unit is similar to that of VTU-1 described by Haman (1992). The device consists of a light, well-balanced pivoting frame with a wind vane attached. The front part of the frame is a thin, suitably shaped rod, which acts as an antidroplet shield and mechanical protector for the fine-wire sensing element. The vane fixes the position of the shielding rod upwind with respect to the local instantaneous flow. The whole instrument is located in an aerodynamically undisturbed place on the aircraft, preferably on a boom with the shaft of the wind vane directed vertically. There is some evidence that moderate deviations from vertical that can occur in the flight conditions should not affect the protective effects of the shield.

A number of designs of the unit have been tried. The one in operational use at the time this paper was written is schematically shown in Fig. 1. The sensing element (1) is a tungsten resistance wire coated with 9% platinum, 2.5 μm thick, and 5 $\pm$ 0.1 mm long. At room temperature its resistance is about 50Ω, depending on individual manufacturing and mounting differences. Wire ends are soldered to 0.3-mm Teflon-insulated copper supports (2), contained in 0.8-mm stainless-steel tubes (3). The sensing wire is located 6.5 mm behind the rod (4), which protects it against wetting by cloud droplets as well as from destruction by other objects

(insects, sand grains, etc.). The rod is made of a 1.1-mm diameter, stainless-steel tube deformed to a hollow, triangular cross section with the back wall 1.3 mm wide. Three holes (5) in the back wall of the rod permit removal of water collecting behind the rod; it is sucked out by means of a Venturi nozzle (6) attached to the rod. The protective effects of the rod are additionally enhanced by a 0.25-mm-thick nylon thread (7) located 3 mm ahead of the rod. The front side of the rod is coated with silicone to become water repellent, while the back side is made hydrophilic by rubbing with soft chalk in order to facilitate sucking the water out of it. Two copper connectors (8) connect the supports electrically to a three-wire extension line. They are made of soft, flexible wires so that the frame can rotate freely around the stainless-steel shaft (9) on a ballpoint bearing (10). The shaft has two stops (11), which limit its turning angle to about $\pm 40^\circ$ and prevent twisting of the connectors. The remaining mechanical elements of the frame, aimed at making the construction sufficiently stiff, are made of brass or stainless steel. The double-tailed, V-shaped vane (12) is made of stiff, 0.5-mm-thick PVC foil. The aerodynamic characteristics of the vane have not been measured and are not exactly known. The frequency of free oscillation of the vane can be roughly estimated from linear theory to be about 10 Hz at 30 m s^{-1} airspeed. A theoretical estimation of the damping coefficient is more difficult; visual observations of the vane behavior in a wind tunnel (the return to equilibrium from deflected position) suggest that it is aperiodic. In such a case the damping factor for 30 m s^{-1} should be more than 60 Hz (an *e*-folding time of less than 0.0167 s). The three-wire extension line connects the sensor with the electronics box so that the sensing wire becomes a branch of a typical Wheatstone bridge. In the particular unit used by the authors, its primary output was adjustable to about 200, 300, or 400 μV K^{-1} depending on the expected ranges of temperature. The output signal is amplified (200 times) and conditioned with a low-pass filter adjusted to the characteristics of the recording unit in use.

As already mentioned, the construction and geometry of the vane and protecting rod as well as positioning of the sensing wire result mostly from the experience gained with thermocouple sensor VTU-1 (Haman 1992) and its later, improved versions VTU-2 and VTU-3. Efforts at further improving of the sensor are continued.

3. Time constant of the new sensor

The time constant of any contact thermometer is defined as the parameter τ in the heat balance equation:

$$\frac{dT}{dt} = \frac{T_a - T}{\tau}, \tag{1}$$

where T is the sensor temperature, T_a is the ambient air temperature, and t is time. For a unit length of an infinite cylindrical wire, which is a reasonable model of our sensor, this equation becomes

$$\frac{dT}{dt} = \frac{4\kappa \mathrm{Nu}(T_a - T)}{\rho c d^2}, \tag{2}$$

where Nu is Nusselt number, ρ is the wire density, c is the wire specific heat, d is the wire diameter, and κ is the heat conductivity of air. Thus, τ is given by the formula

$$\tau = \frac{cd^2\rho}{4\kappa \mathrm{Nu}}. \tag{3}$$

To estimate τ with a precision of a few percent, we use the values $\kappa = 254.28 \times 10^{-4}$ W K^{-1} m^{-1}, $\rho = 1.95 \times 10^4$ kg m^{-3}, $c = 133.14$J kg^{-1} K^{-1} as sufficiently accurate and disregard their dependence on temperature or other factors. For the Nusselt number we apply one of the widely accepted empirical formulas (Fand and Keswani 1972):

$$\mathrm{Nu} = 0.184 + 0.324\ \mathrm{Re}^{0.5} + 0.291\ \mathrm{Re}^{Y},$$
$$Y = 0.247 + 0.0407\ \mathrm{Re}^{0.168}, \tag{4}$$

where $\mathrm{Re} = vd/\nu$ is Reynolds number, ν is air kinematic viscosity, and v is air velocity. Varying ν within (1.46–2.03) $\times 10^{-5}$ m^2 s^{-1} (which corresponds to the height range 0–4000 m of an ICAO standard atmosphere), we find that for the range of velocities 25–100 m s^{-1} the Nusselt number should vary within the limits 1.16–2.23. This yields values of τ in the range (0.71–1.37)$\times 10^{-4}$ s.

Verification of the latter result by direct measurement in a wind tunnel or in flight is a complicated task. It is difficult to create thermal impulses in the airflow of a shape suitable for determination of such a small time constant. To circumvent this difficulty, we used the technique similar to that used by Lenschow (1972), that is, varying the temperature of the sensor instead of temperature of the air. The sensor was installed in a wind tunnel and the sensing wire was periodically heated with carefully shaped ''top-hat'' impulses of electric current of about 4-ms duration, separated by 8-ms periods. The relaxation of the thermometer during the pause in heating has been recorded on a digital recording voltmeter with sampling frequency 50 kHz, (in volts, without rescaling to kelvins). The relaxation curve has been approaching an asymptotic value 0.63 V, which resulted from incidental offset of the electronic circuit. It was found that this curve can be nearly ideally fitted with the following function $\Phi(t)$ (see Fig. 2):

$$\Phi(t) = -1.21 \exp\left(\frac{-t}{\tau_1}\right) - 0.33 \exp\left(\frac{-t}{\tau_2}\right) + 0.63. \tag{5}$$

The first time constant $\tau_1 = (3.94 \pm 0.14) \times 10^{-5}$ s can be identified as reflecting the electric properties of the electronic circuit and is practically irrelevant. The second one, τ_2, represents the true thermal response of

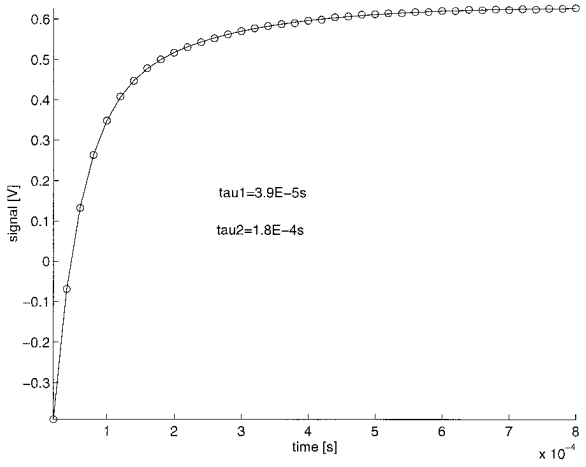

FIG. 2. Response of the UFT sensor to the steplike change of its temperature at 30 m s^{-1} ventilation speed in a wind tunnel. Circles—measured values of the UFT output in volts versus time; solid line—the best fit with a linear combination of two exponential functions as in Eq. (5).

the sensor. At ventilation speed of 30 m s^{-1} $\tau_2 = (1.86 \pm 0.19) \times 10^{-4}$ s; experiments at 20 and 40 m s^{-1} gave $\tau_2 = (2.18 \pm 0.23) \times 10^{-4}$ and $\tau_2 = (1.68 \pm 0.17) \times 10^{-4}$ s, respectively. These results are in a reasonable agreement with the theoretical values computed according to (3).

The effective response of UFT may depend also on the thermal influence of the supports and protecting rod. These effects were not accounted for with this method and had to be determined in another way. The effect of the supports created no major problems. With the length-to-diameter ratio of about 2000, it could simply be ignored (Paranthoen et al. 1982). The effect of the protecting rod requires more attention, being important not only for the inertia of the sensor, but also for its accuracy and resolution. It was estimated on the basis of wind tunnel tests, similar to those performed when testing the VTU-1 thermocouple sensor (Haman 1992). For these tests, a special vane was prepared in which the protecting rod could be electrically heated. In the first series of tests a small thermocouple was attached to the rod, and the dependence of its temperature increase with respect to the heating current and ventilation speed was established. The thermocouple was then removed (in order to avoid possible disturbances of the flow around the rod) and the rod was periodically heated by impulses of electric current, long enough to permit stabilization of the rod's temperature during each impulse at a level of few kelvins above the ambient value; this level was determined from the airspeed and heating current, on the basis of previous tests. Here ΔT_S, the difference in temperature measured by the sensor between the ''heated'' and ''unheated'' regimes related to ΔT_R, the respective temperature difference of the rod, is a measure of the rod's thermal influence. During these tests it was found that $\Delta T_S/\Delta T_R$ is 2%–3%, practically independent of the ventilation speed in the range 10–40 m s^{-1}. In real atmospheric conditions the difference between the temperature of the rod and the ambient air can seldom exceed 2–3 K, so the resulting error will usually be below 0.1 K; as will be seen later, this is below the practical resolution of the instrument.

Let us now return to the problem of the influence of thermal inertia of the protecting rod on the overall inertia of the sensor. The thermal time constant of the rod has been determined by measurements in the wind tunnel and found to be about 1 s for ventilation speeds of 30–40 m s^{-1}. It is four orders of magnitude greater than that of the sensor. One can show that in the case of such a great difference between these constants, the resultant thermal relaxation curve $\Phi(t)$ of the instrument can be represented as a linear combination of two exponential functions of the form:

$$\Phi(t) = A_S \exp\left(\frac{-t}{\tau_S}\right) + A_R \exp\left(\frac{-t}{\tau_R}\right), \qquad (6)$$

where τ_S and τ_R represent the time constants of the sensor and the rod, respectively. It is easy to see that $A_S/A_R = \Delta T_S/\Delta T_R$. This means that input of the thermal inertia of the protecting rod into the resultant relaxation of the instrument will again be about 2%–3%, giving effects below the available resolution. This is also much less than the effects of housings of other types of immersion airborne thermometers (Friehe and Khelif 1993).

4. Resolution of the UFT

The resolution (relative accuracy) of the UFT is limited mostly by the noise, which increases with the aircraft velocity. At low speeds, up to 40 m s^{-1}, the amplitude of this noise does not exceed 0.15 K. This has been tested in the wind tunnel at various airspeeds in the range of 25–40 m s^{-1}, at sampling frequencies of 20 and 50 kHz. The noise of the larger amplitude is visible on the in-flight records taken at a 10-kHz rate with a 5-kHz low-pass, second-order Butterworth filter; the flights were made on the Do-228 aircraft at airspeeds of 60–100 m s^{-1} (120–195 kt). The root-mean-square level of this noise varies from 0.09 K at 60 m s^{-1} to 0.37 K at 100 m s^{-1}; its maximum amplitudes are up to three times higher. Representative examples of the records are shown in Fig. 3 for two time resolutions and are additionally illustrated by their Fourier spectra in Fig. 4. Visual inspection of the records reveal that the smallest typical timescale of the noise is of about 10^{-3} s, but a few longer scales can also be seen. The nature of this noise is not well understood yet, but some attempts at its explanation can be nevertheless made. First, part of the noise may be due to the generation of microturbulence by the protective rod and the oscillations of its wake, connected with vortex shedding. The Strouhal number for a triangular rod is not exactly

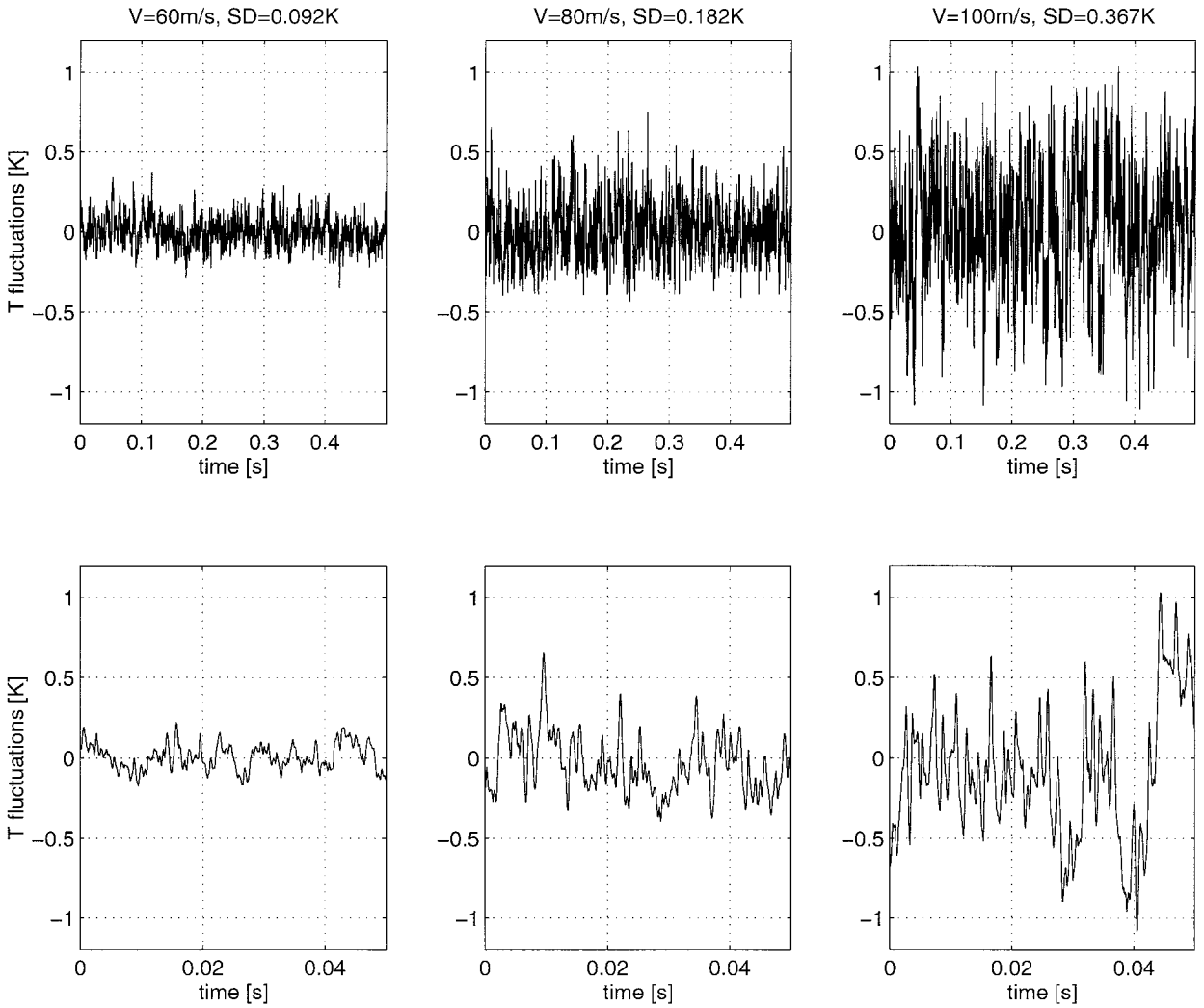

FIG. 3. The examples of temperature fluctuations at various airspeeds in horizontal flight in clear air recorded on the Do-228 aircraft. Records are made with 10-kHz sampling frequency, after conditioning with a 5-kHz low-pass filter and presented in two time resolutions (upper and lower plots). Speed and standard deviation of temperature fluctuations are given in plot titles.

known, but presumably is of the order of 10^{-1}, which suggests a shedding frequency of about 10 kHz; however, in the Fourier transform no clearly dominating frequency can be found.

On the Do-228 aircraft, part of the noise may be due to the turbulence generated by flow around some elements of the aircraft body; the fact that Fourier transform of the noise contains frequencies much lower than those following from the above eddy shedding estimate and is evidently different from the typical atmospheric ''$-5/3$'' line (observed with this sensor mounted on the nose boom of the ''Ogar'' motorglider) seems to substantiate this supposition. For technical reasons the instrument had to be mounted under the central part of the fuselage of Do-228. This was not ideal for avoiding aerodynamical disturbances, so it is possible than in another place the level of the noise could perhaps be lower.

The possibility that part of the noise results from rapid quasi-periodic deflections of the vane that can follow from its natural oscillations has been tested in the wind tunnel by fixing the vane at various angles with respect to the flow and looking at the corresponding level of the noise. The angle has also been varied in a continuous manner from full exposure of the unprotected sensing wire on one side of the vane to full exposure on the other (Fig. 5). One can see that the noise level recorded with the unprotected wire is about three times lower than that when the sensor was placed behind the rod. Notice that in the latter position the value of total temperature is considerably lower than for unprotected wire; we shall return to this feature later. Noise on the unprotected wire results presumably from temperature and velocity fluctuations in the natural turbulence of the tunnel flow. The sharp ''V''-shaped distribution of dynamic heating in the function of the deflection angle

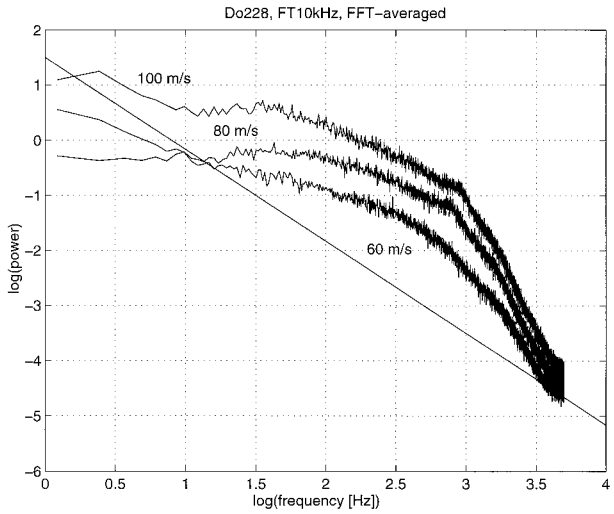

FIG. 4. Power spectra of the records which examples are shown in Fig. 3. The solid line is a reference with a −5/3 slope.

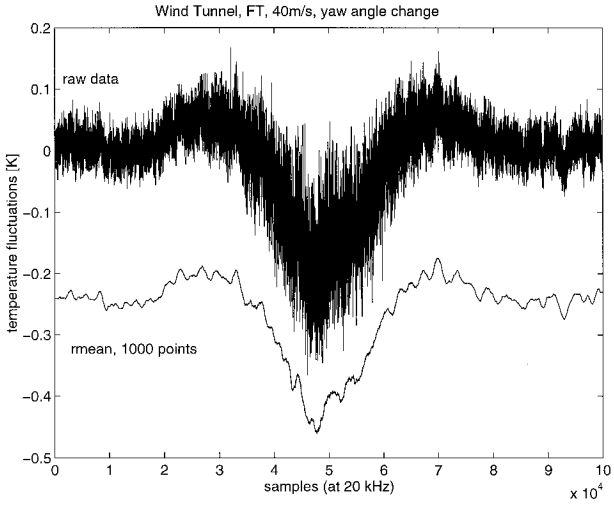

FIG. 5. Temperature fluctuations recorded in a wind tunnel during continuous rotation of the sensor with respect to the direction of the airflow. Wind speed 40 m s^{-1}. Width of the V-shape on the plot corresponds to the change of the yaw angle from about −2° to about +2°. The raw data are given in the upper plot; the lower plot is a 1000-point running mean of the upper plot displaced 0.25 K downward.

suggests that a certain part of the noise may result from small oscillations of the vane in turbulent flow.

There were suspicions that part of the noise may be due to the strain effects of the vibrating, relatively long wire, though tungsten is known to be very resistant to stretching. To check this hypothesis, the sensor has been moved through a small basin filled with vegetable oil, with speeds up to about 5 cm s^{-1}. The hydrodynamic strain connected with such motion is equal to that which corresponds to an air velocity of up to about 200 m s^{-1}. The effects, if any, corresponded to less than 0.02 K, about the thermal inhomogeneity in the oil. This means that strain effects can be neglected, when compared with thermal effects.

Resolution of temperature measurement with UFT can be in some cases improved at the expense of resolution in time, by suppressing the noise with suitable smoothing. Because of the relatively high frequency of the noise, the resulting loss of small-scale details may still be tolerable. An example of such a procedure is presented in Fig. 6. A fourth-order Butterworth low-pass filter with a 50-Hz cutoff frequency is numerically applied to a 10-kHz record and then resampled with a 200-Hz rate, simulating a slower but still relatively fast recording system. Despite the evident reduction of the effective response speed, the instrument remains nevertheless faster than other kinds of airborne thermometers.

The applicability of the presented instrument depends on the requirements on its performance with respect to particular aims of measurements. Looking for temperature variations of the order of 1 K, one can accept ±0.15-K resolution. In such a case, installation of the UFT on an aircraft able to operate at speeds below 40 m s^{-1} is fully justified. Nevertheless efforts aimed at suppressing the noise also at higher velocities by modification of the instrument geometry have been undertaken.

5. Recovery factor of the UFT

At present, the recovery factor of the UFT is known only with relatively low accuracy, as there was no possibility to measure it directly. The range of velocities in the wind tunnels available to the authors is too small for that purpose, and there have been no suitable conditions to do it in flight. An indirect estimate can be obtained by considering the recovery factor of the thermocouple VTU-1 sensor (Haman 1992), which has similar geometry; its value has been roughly estimated as 0.4 ± 0.1 for speeds of about 30 m s^{-1} and has been later confirmed for speeds up to 90 m s^{-1} during flight tests on the Do-228.

Another estimate of the recovery factor for wind tunnel conditions can be obtained assuming that its value for an unprotected wire is close to the square root of the Prandtl number, which for air is about 0.83. Denoting by ΔT the difference of temperature between the protected and unprotected position of the sensing wire for smoothed records in Fig. 5, we can estimate the recovery factor r from the formula

$$r = 0.83 + \frac{2\Delta T c_p}{v^2}, \tag{7}$$

which after substituting appropriate values for the airspeed v gives $r \approx 0.6$ for the wind tunnel speeds. Both these values are relatively low, but this can be understood looking again at Fig. 5. It reveals that there is a visible fall of total temperature behind the protective

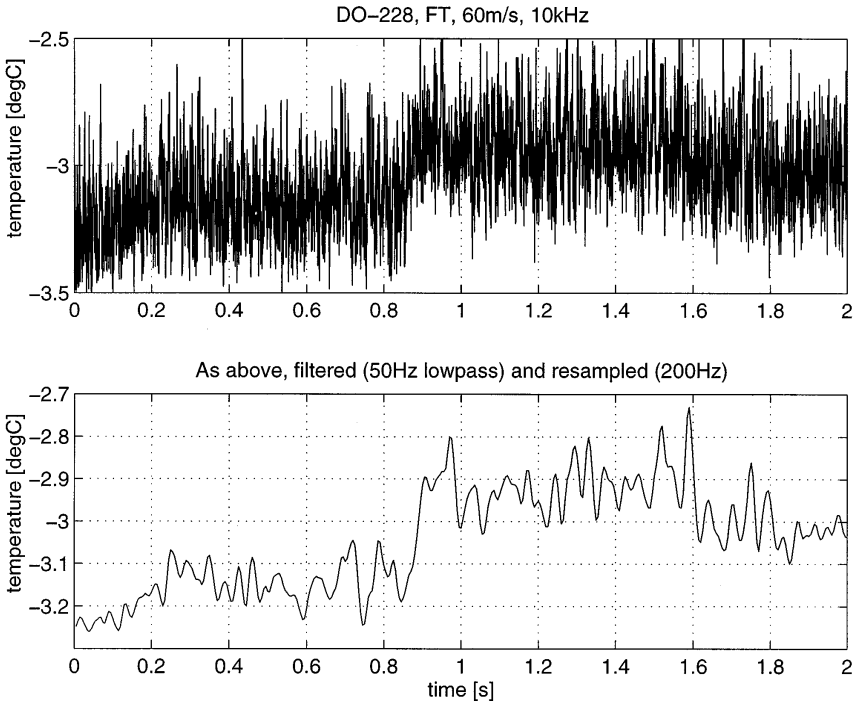

FIG. 6. Upper curve: a section of the record from Do-228 (collected in the same way as examples in Fig. 3). Lower curve: the same section after conditioning with 50-Hz low-pass, fourth-order Butterworth filter and resampling with 200-Hz frequency.

rod with respect to that of an unprotected wire. This fall may be due to the reduction of pressure in the wake of the protective rod as well as due to a reduction of velocity. From experiments with a liquid water content meter that uses similar protection but that has compensation for the airspeed reduction by means of the Venturi effect, it was estimated that this velocity is reduced to about 60% of the undisturbed value (Haman et al. 1992). On the other hand, preliminary attempts at computer simulations of the flow behind the protective rod suggest the presence of small transient eddies with considerable pressure and temperature depressions that quasi-periodically pass close to the sensing wire and can give short impulses of relatively low temperature. Although there are some doubts as to what extent those simulations are realistic, such an effect is possible and may contribute to diminishing the resultant dynamic heating. Efforts at more precise determination of the recovery factor and its possible dependence on air velocity are being continued.

6. Accuracy of the UFT

Accuracy of any instrument is determined (or rather limited) by superposition of errors generated by all various factors affecting its operation. Disregarding possible effects of wrong placement of the instrument on the aircraft, the most important source of errors of the UFT are the fluctuations of the temperature records attributable to microturbulence behind the protective rod, depending on aircraft velocity (as discussed in section 4); for instance, for the motorglider speeds (25–30 m s^{-1}) their level has been found to be about ± 0.1 K. Relative to them other errors seem to be of secondary importance. Errors resulting from thermoelectric effects between the sensing wires and copper connectors should not exceed 0.03 K. The radiation errors for such a fine wire are negligible as are the thermal effects of the supports, discussed earlier (1:2000 diameter-to-length ratio). The possible error due to the thermal influence of the protecting rod has been estimated in section 3 as usually less than 0.1 K. Thus, ± 0.2 K seems to be a safe estimate of the relative accuracy (resolution) of the sensor at least at the low speeds of a motorglider.

The absolute accuracy of the instrument additionally depends on the stability of the sensor, the electronics and the quality of the calibration. There are no basic problems with building the electronics and performing calibration at a level that would yield errors much below the practical resolution of the instrument. Concerning the stability of the sensor, in some cases slow drift of calibration curves toward higher resistances has been observed. Its causes remain unclear. The most probable seems corrosion of tungsten due to damage of the platinum coat; thus, efforts have been undertaken toward improving the manufacturing technology and better protection of the platinum coating against possible damage. Absolute accuracy of the instrument will be additionally

affected by uncertainty of determination of the recovery factor in degree depending on the airspeed. At present, for a motorglider flying about 30 m s^{-1}, this error does not exceed ± 0.2 K.

The above estimates of the UFT accuracy assume perfect efficiency of the antiwetting protection. Malfunctioning of this device resulting in wetting of the sensor by cloud droplets may yield two kinds of false signals. First, after leaving the cloud the wet sensor indicates the wet-bulb temperature of the surrounding air (or something between wet-bulb or dry-bulb temperatures in the case of partial wetting), which can be even a few kelvins lower than the actual one. This gives characteristic negative disturbances in the record. On the other hand, mixing and evaporative cooling on the edges of the cloud may give similar effects in real temperature, which can make identification of sensor wetting in such a case uncertain. The second kind of error results from applying the usual correction for dynamic heating of a dry sensor to a wet one (Lawson and Cooper 1990). For good correction one should assume that in the case of a wet sensor the conversion of the kinetic energy to internal energy of air goes wet, not dry, adiabatically. This means that the correction for the dry sensor should now be multiplied by the ratio of wet to dry adiabatic lapse rates. In typical summer conditions, this ratio may be 0.5 or even less. The resulting error depends on the recovery factor and the degree of wetting of the sensor, but for the low speed of a motorglider (30 m s^{-1}) will not exceed 0.2 K and may be hidden in the other kinds of noise. However, for speeds of about 100 m s^{-1} it may become 2 K or even more.

Efficiency of our antidroplet protection seems good, though at present we cannot state this with 100% certainty. In the case of such a fine sensor we found no practical method for evaluating this efficiency in a direct way. Observations and photographs in a wind tunnel at speeds 25–40 m s^{-1} with the water spray corresponding to LWC up to 5 g m^{-3} have shown that the water collected by the protecting rod is being effectively removed and no visual or electric signs of wetting of the sensing wire could be noticed. Also during the test flights, no indirect signs of wetting in the form of characteristic disturbances in temperature after leaving the cloud were observed, which means that either no wetting took place or drying lasted too briefly to be detected by the recorder (an example of such a situation is presented in the next section). This may, however, depend on the particular shape of the droplet spectrum; thus, more observations made in various conditions should be collected before a more definite statement in that respect could be made. On the other hand, certain experiments performed recently in the laboratory conditions seem to uphold the supposition that in the case of such a fine wire, the cloud droplets that accidentally hit it are unable to stick to it and make it wet. As it is very important for further development of the instrument, this problem is now under intensive investigation.

Accounting for all these uncertainties, we suggest that until they are eliminated, the UFT instrument should be mostly used on a small aircraft as a sensor of local fast fluctuations in temperature with another, slower but more reliable, thermometer as a reference for absolute values.

7. Examples of some experimental measurements in clouds

In 1994 two flights aimed at making observations in small cumulus clouds were made in the vicinity of Warsaw, Poland, on 23 and 25 August. Their results are described in detail in a separate paper (Haman and Malinowski 1996); here only a few examples are presented as an illustration of the capabilities of the new instrument. The aircraft was a motorglider SZD 45 Ogar, flying at a cruising airspeed of about 28–30 m s^{-1}. It was equipped with one UFT and with a thermocouple sensor VTU-3 [modified version of the VTU-1 described by Haman (1992) with a 50-μm chromel-constantan thermocouple]. Both instruments were located close to each other (about 25 cm separation side by side) on a nose boom 1 m long (Fig. 7). Unfortunately, an experimental version of VTU-3 used in this flight appeared vulnerable to wetting. Additionally there was a failure in the connecting line in the VTU that resulted in variation of the baseline of the record after entering the cloud. Thus, the comparison of these two thermometers appeared possible only to a limited extent. For technical reasons a recorder of poorer performance than that on the Do-228 had to be used; the measurements were digitally recorded with a 999-Hz sampling frequency on a 12-bit recorder, which represents a resolution of 0.02 K bit^{-1} for the VTU and 0.04 K bit^{-1} for the UFT. The VTU output was recorded with the 3-Hz cutoff frequency low-pass filter; for the UFT the records were made on two channels: with 3- and 300-Hz filtering. In Fig. 8a, these three records taken during a pass through a cloud at 2200-m altitude (about 400 m above the cloud base) are shown. Edges of the cloud appear as a sharp fall of the temperature with the respect to the environmental values at the beginning and the end of the record, as well as in short interval around 12–15 s. The segment between 40 and 44 s corresponds to the evident wetting of the VTU sensor with UFT sensor remaining dry. The response of the sensors between 40 and 42 s is in the opposite phases: Wet VTU shows the drop of the temperature (evaporative cooling) in the segments of higher environmental air temperature indicated by UFT, following is slow drying of the VFT sensor (43 and 44 s). Figures 8b and 8c present selected fragments of this pass with enhanced time resolution. Again segment between 12 and 12.1 s corresponds to the dry UFT and wet VTU. In general, good agreement between the ''3-Hz'' records of both thermometers is visible except for the wetting of the VTU in cloud. A small phase shift between these records results from differences in inertia

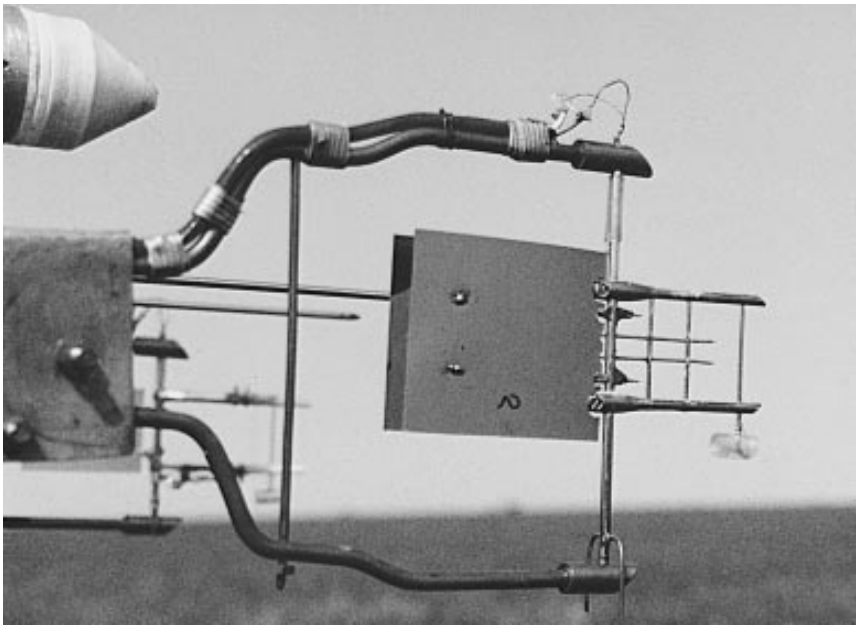

FIG. 7. UFT sensor mounted on the nose boom of the SZD-45 OGAR motorglider. The 5-mm length of the sensing wire may serve as a scale.

of the sensors, which are not completely canceled by filtering, while other minor differences may reflect a difference in the location of the sensors. The 300-Hz record reveals a number of decimeter scale features that are completely lost by the slower instrument. It is worth noticing that the noise level of these 300-Hz records usually does not exceed ± 2 bits, that is, less than ± 0.1 K. Particularly noticeable is a jump of more than 1.2 K over a distance of about 10 cm, visible at 11.852 s of the record. A number of such jumps, both positive and negative, with amplitudes sometimes exceeding 2 K, were found during this flight. Though the presence of such a phenomena could be anticipated on the basis of results by Baker (1992), Brenguier (1993), and others, empirical confirmation of their existence illuminate possible effects of entrainment and mixing in cumulus clouds.

8. Closing remarks

Although experience with the UFT instrument is rather limited yet, some remarks can be nevertheless made.

Most of the test flights with the UFT sensors have been made on an Ogar SZD-45 motorglider with a cruising speed of about 30 m s^{-1}. A few short flights were made on a turboprop Do-228 and on a Falcon jet from the DLR aircraft facility in Oberpfaffenhofen, Germany, with airspeeds ranging from 60 to 200 m s^{-1} aimed mostly at checking if the very delicate sensor can even survive usage on a fast aircraft and what sort of unexpected problems may appear.

During flights on the motorglider the sensor performed well. Despite its fineness, the sensing wire survived more than 15 h in the air as well as a number of takeoffs and landings from a grass field. A greater danger than mechanical damage appears to be particles and fibers (e.g., fragments of spiderwebs), which occasionally stick to the sensing wire during taxiing; they can dramatically increase the inertia of the sensor and are practically impossible to remove without damaging the wire, so that exchange of the sensor becomes the only solution. Typical disturbances resulting from the presence of hygroscopic particles (Schmitt et al. 1978) may also occur; thus, the sensing wire should be carefully rinsed with distilled water before each flight.

During flights on the Do-228 the UFT also performed fairly well, except for the relatively high level of turbulent noise that occurred at greater speeds. In one flight the wire was broken in heavy rain; however, this happened during a steep turn, with a relatively large roll angle, when the rod might give insufficient protection against large objects falling fast. An alternative explanation is unusually strong oscillations of the vane hit by a heavy droplet and then exposing the sensing wire to an another one.

On the Falcon the sensor had to be located under the fuselage, and special measures have been taken in order to protect the sensor against the impact of small objects shedded by the front wheel during takeoff. The sensing wire eventually was broken in clear air at temperature below -20°C, presumably because of thermal strain (it has only been tested down to -12°C after manufacturing). Another wire, which was relatively loose, was broken (presumably because of vibrations) shortly after takeoff. This means that precise adjustment of the wire tension may be critical, if the sensor is to be used at higher speeds and in a wide range of temperatures.

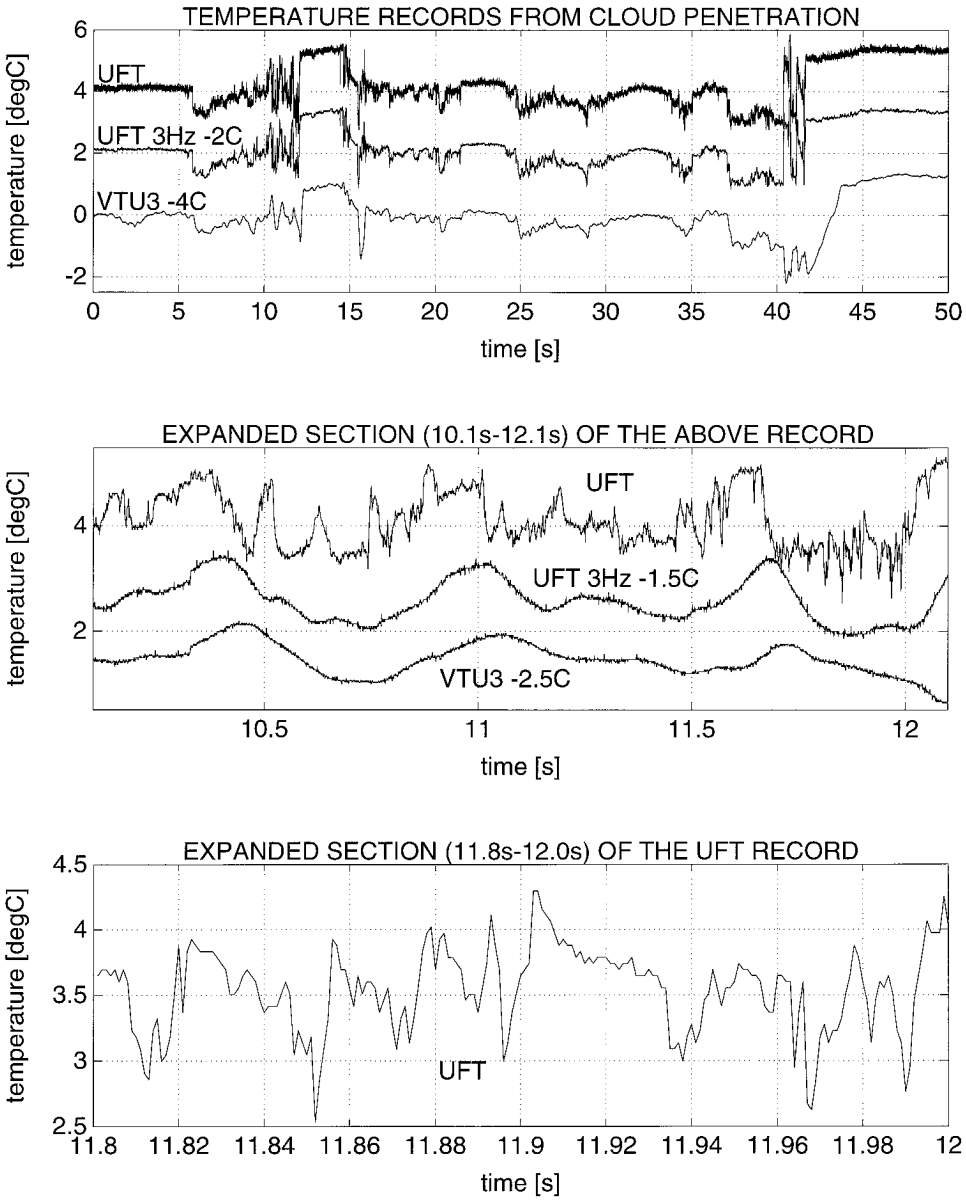

FIG. 8. Examples of temperature records from penetration of a small cumulus cloud. Motorglider SZD-45 Ogar, speed about 30 m s^{-1}, sampling rate 999 Hz (one sample corresponds to about 3 cm). Record starts at 5 s (150 m) before entering the cloud. Time in seconds from the beginning of record. (a) the whole record; (b, c) time-expanded fragments; (a) and (b) upper record (fast): UFT, conditioned with the 300-Hz low-pass filter; (a) and (b) middle record (slow): UFT, conditioned with the 3-Hz low-pass filter, displaced downward for better presentation; (a) and (b) bottom record (VTU-3): VTU-3 conditioned with the 3-Hz low-pass filter, displaced downward for better presentation; (c) UFT, conditioned with 300-Hz low-pass filter. Notice a jump of more than 1.2 K over about 10-cm distance (4 samples) at 11.852 s as well as other structures at scales of a few centimeters.

It has already been mentioned that some efforts have been undertaken to make a computer simulation of the airflow pattern and droplet trajectories around the protective rod and the sensor. Unfortunately, the problem is very expensive in terms of CPU time, so only few simulations, permitting no definite conclusions (even with respect to the correctness of the model) have been made until now. However, these results have already yielded certain suggestions with respect to possible further improvements aimed at reducing the level of the noise discussed in section 4.

9. Conclusions

In its present configuration, the UFT is already an effective tool for measuring temperature fluctuations in

clouds with spatial resolution down to the centimeter scale. It is not free, however, from certain limitations and drawbacks. The main one is a high-frequency noise in the temperature, caused by airflow disturbances behind the antidroplet shield. The level of this noise is tolerable at low velocities up to 40 m s^{-1} but is excessive at higher speeds. Efficiency of the antidroplet protection seems to be good at the low airspeeds but is not established yet with absolute certainty. It is also not clear to what extent the instrument is vulnerable to icing and large precipitation particles, which may limit its applicability to warm nonraining clouds. Nevertheless, we hope that even with those limitations the instrument may open new areas for experimental research in cloud thermodynamics and dynamics.

Acknowledgments. This research is a result of cooperation between the Atmospheric Physics Division of the Institute of Geophysics, University of Warsaw, Poland, and the Institute of Atmospheric Physics, DLR, Oberpfaffenhofen, Germany, under the Polish–German Governmental Agreement on Scientific Cooperation. It was also supported by Grant 6 6314 91 02 of the Polish Committee for Scientific Research.

The authors are indebted to their colleagues from the Institute of Geophysics, University of Warsaw, Poland, and from the Institute of Atmospheric Physics, DLR, Germany, for their assistance and many inspiring discussions, as well as to the aircraft crews. Assistance of Mr. D. Meyr, W. Dietrich, H. Löbel, and H. Horst is particularly acknowledged. Numerical experiments performed by Dr. Wanda Szyrmer from Université du Quebéc a Montreál, Canada, were of great help during development of the instrument. Remarks of Dr. Paul Lawson and anonymous reviewers helped much at improving the final version of the paper.

REFERENCES

Baker, B., 1992: Turbulent entrainment and mixing in clouds: A new observational approach. *J. Atmos. Sci.,* **49,** 387–404.

Baumgardner, D., B. Baker, and K. Weaver, 1993: A technique for the measurement of cloud structure on centimeter scales. *J. Atmos. Oceanic Technol.,* **10,** 557–565.

Brenguier, J. L., 1993: Observation of cloud structure at the centimeter scale. *J. Appl. Meteor.,* **32,** 783–793.

Fand, R. M., and K. K. Keswani, 1972: A continuous correlation equation for heat transfer from cylinders to air in crossflow for Reynolds numbers from 10^2 to 2×10^5. *Int. J. Heat Mass Transfer,* **5,** 559–561.

Friehe, C. A., and D. Khelif, 1993: Fast-response aircraft temperature sensors. *J. Atmos. Oceanic Technol.,* **10,** 784–795.

Fuehrer, P. L., C. A. Friehe, and D. K. Edwards, 1994: Frequency response of a thermistor temperature probe in air. *J. Atmos. Oceanic Technol.,* **11,** 476–488.

Grabowski, W. W., 1993: Cumulus entrainment, fine scale mixing and buoyancy reversal. *Quart. J. Roy. Meteor. Soc.,* **119,** 935–956.

Haman, K. E., 1992: A new thermometric instrument for airborne measurements in clouds. *J. Atmos. Oceanic Technol.,* **9,** 86–90.

——, and H. Pawlowska, 1995: Dynamics of nonactive parts of convective clouds. *J. Atmos. Sci.,* **52,** 519–531.

——, and S. P. Malinowski, 1996: Temperature measurements in clouds on a centimeter scale—Preliminary results. *Atmos. Res.,* **41,** 161–175.

——, A. M. Makulski, and S. P. Malinowski, 1992: A new LWC-meter for slowly flying aircraft. *Proc. 11th Int. Conf. on Clouds and Precipitation,* Vol. 2, Montreal, PQ, Canada, International Commission on Clouds and Precipitation and International Association of Meteorology and Atmospheric Physics, 956–957.

Lawson, R. P., and W. A. Cooper, 1990: Performance of some airborne thermometers in clouds. *J. Atmos. Oceanic Technol.,* **7,** 480–494.

——, and A. R. Rodi, 1992: A new airborne thermometer for atmospheric and cloud physics research. Part I: Design and preliminary flight test. *J. Atmos. Oceanic Technol.,* **9,** 559–574.

Lenschow, D. H., 1972: The measurement of air velocity and temperature using the NCAR Buffalo aircraft measuring system. NCAR Tech. Note TN/EDD-74, 39 pp. [Available from National Center for Atmospheric Research, P.O. Box 3000, Boulder, CO 80307-3000.]

Malinowski, S. P., M. Y. Leclerc, and D. G. Baumgardner, 1994: Fractal analysis of high resolution cloud droplet measurements. *J. Atmos. Sci.,* **51,** 387–413.

Marillier, A., M. Cabane, and D. Cruette, 1991: ·Preliminary tests of an ultrasonic thermoanemometer for aircraft measurements. *J. Atmos. Oceanic Technol.,* **8,** 597–605.

McCarthy, J., 1973: A method for correcting airborne temperature data for sensor response time. *J. Appl. Meteor.,* **12,** 211–214.

Nacass, P. L., 1992: Theoretical errors on airborne measurements of: static pressure, impact temperature, air flow angle, air flow speed. NCAR Tech. Note TN-385+STR, 61 pp. [Available from National Center for Atmospheric Research, P.O. Box 3000, Boulder, CO 80307-3000.]

Paranthoen, P., C. Petit, and J. C. Lecordier, 1982: The effect of the thermal prong-wire interaction on the response of a cold wire in gaseous flows (air, argon and helium). *J. Fluid Mech.,* **124,** 457–473.

Rodi, A. R., and P. Spyers-Duran, 1972: Analysis of time response of airborne temperature sensors. *J. Appl. Meteor.,* **11,** 554–556.

Rosemount, 1963: Total temperature sensors. Rosemount Engineering Company Bull. 7637, 27 pp.

Schmitt, K. F., C. A. Friehe, and C. H. Gibson, 1978: Humidity sensitivity of atmospheric temperature sensors by salt contaminations. *J. Phys. Oceanogr.,* **8,** 151–161.

Shaw, W. J., and J. E. Tillman, 1980: The effects of and correction for different wet-bulb and dry-bulb response in thermocouple psychrometry. *J. Appl. Meteor.,* **19,** 90–97.